MEASUREMENT OF RADIATIVE NON-EQUILIBRIUM FOR AIR SHOCKS BETWEEN 7-9 KM/S

Brett A. Cruden[(1)], Aaron M. Brandis[(1)]

[(1)] AMA Inc at NASA Ames, NASA Ames Research Center, MS 230-2, Moffett Field, CA 94035, E-mail:Brett.A.Cruden@nasa.gov, Aaron.M.Brandis@nasa.gov

ABSTRACT

This paper describes a recent characterization of non-equilibrium radiation for shock speeds between 7 and 9 km/s in the NASA Ames Electric Arc Shock Tube (EAST) Facility. Data is spectrally resolved from 190-1450 nm and spatially resolved behind the shock front. Comparisons are made to DPLR/NEQAIR simulations using different modelling options and recommendations for future study are made based on these comparisons.

1. INTRODUCTION

In recent years, extensive campaigns have been conducted to measure radiation in air shocks at velocities from 9-15 km/s.[1] However, little recent data exist characterizing the radiation characteristics below this velocity range. Although the radiative heat flux magnitude in this velocity region is relatively small, around 10% of the radiative heat load may originate from velocities less than 9 km/s for lunar return. For entries from low earth orbit, it comprises the entirety of radiative heating. Therefore, a test series has been undertaken in the EAST facility to characterize this range, the results of which are reported here. Experiments were undertaken in the 7-9 km/s velocity range, at six different freestream pressures from 0.01-0.70 Torr. Simulations of these experiments were carried out with the DPLR and NEQAIR codes with 12 different modelling options. The amount of data (measured and simulated) is voluminous, so only a subset of results is presented in order to draw general conclusions about the state of predictive modelling.

2. EXPERIMENTAL

The EAST facility has been described in detail in previous work [2]. A 1.2 MJ, 40 kV capacitor bank drives one of two shock tubes. The first is a 60.33 cm inner diameter stainless steel tube, intended for testing at low density, and the second is a 10.16 cm aluminum tube which has been extensively utilized in high velocity testing in recent years. The observation section is located 21.4 m downstream of the diaphragm in the 60 cm tube and 7.9 m downstream in the 10 cm tube. The radiance is imaged axially onto a collection of four spectrometers, producing spectrally and spatially resolved radiance data in each test. On the 60 cm tube, two spectrometers are simultaneously in use, while four spectrometers are used simultaneously on the 10 cm tube. Between these spectrometers, radiance is measured from 190-540 nm and/or 480-1450 nm with each test.

Tests in the 60 cm tube were conducted with initial pressures of 0.01, 0.05 and 0.14 Torr, while the 10 cm tube was employed at pressures of 0.14, 0.30, 0.50 and 0.70 Torr. The velocities spanned 6.8-9.2 km/s, with higher velocities generally being tested at lower pressures. A total of 51 tests were conducted, 33 of which were performed in the 24" tube. Tests with triggering errors, insufficient test time (<2 μs) or unusual shock structure were discarded, leaving 44 with acceptable data quality. For each of the six pressures examined, one representative test is selected for further analysis. In order to provide analysis at all wavelengths and on both tubes, this requires 10 shots to be analyzed. The conditions of the shots are shown in Table I below.

Table I. Shot Conditions presented in this work

Shot No	Velocity (km/s)	Pressure (torr)	Range (nm)	Tube Diameter (cm)
15	8.18	0.01	190-500	60.33
32	8.57	0.01	500-1450	60.33
8	8.62	0.05	190-500	60.33
24	8.87	0.05	500-1450	60.33
20	8.29	0.14	190-500	60.33
22	8.36	0.14	500-1450	60.33
38	8.33	0.14	190-1450	10.16
42	8.09	0.3	190-1450	10.16
46	7.71	0.5	190-1450	10.16
50	7.34	0.7	190-1450	10.16

3. ANALYSIS

In order to simulate these results, it is assumed that the shock tube measurements show similarity to the stagnation line over a blunt body. A 3-m sphere is

simulated using DPLR v4.04.0. The stagnation line is then passed to NEQAIR15, which is run in "shock tube" mode (i.e. radiance calculated perpendicular to the line-of-sight direction) to create a radiation profile along the tube axis. Different modelling options are explored in order to investigate their impact on the radiance.

The first option involves the manner in which electron and electronic energy are accounted for within the context of the two-temperature model. Traditionally, DPLR has assumed energy stored in these modes to be determined by a combined translational-rotational-electronic temperature, with a separate temperature used to describe vibrational energy. In contrast, other codes such as LAURA have assumed the vibrational and electronic modes to be lumped. The traditional DPLR approach poses a difficulty for radiation solutions as the large translational temperatures obtained in thermal non-equilibrium result in excessive radiation from electronic states. The solution had been to set the electronic temperature to the vibrational temperature when the DPLR stagnation line was parsed to the radiation code, even though it was inconsistent with the way the CFD solution was run. DPLR v4.04.0 now provides an option to simulate the energy partition with a lumped vibrational-electronic temperature, thus removing the need for the above workaround.

The second option is the chemical kinetic model used to produce the chemical non-equilibrium solution. Traditionally, the rates published in Park's 1990 text have been employed by NASA flight projects.[3] In 1993, Park published an update to these rates which is also run in this work.[4] The third chemistry model uses the rates employed by Johnston in 2014[5], which are the rates currently used with the LAURA CFD code. These rates are largely based on the work of Park, though some have been modified based on recent studies. A summary of the differences in the three rate models is given in Table II. Eleven reactions that are the same in all three models are omitted from the table. It is seen that six rates were altered from Park90 to Park93 while Johnston employs ten different rates from Park90. An additional variation exists in the controlling temperature for associative ionization processes. It has long been standard practice in the two temperature model to use $\sqrt{TT_v}$ as the controlling temperature for dissociation reactions and T as the controlling temperature for other reactions. Reactions that involve electron impact might be expected to be controlled by T_e, however the existing formulation of DPLR does not allow this. A modified version of DPLR was run which allowed dissociative recombination (i.e. the reverse of associative ionization) to be controlled by T_e, but this had little impact.

Table II. Summary of differences in kinetic rate models, by source

Reaction	Park 90	Park 93	Johnston 2014
$NO + M \leftrightarrow N + O + M$	[3]	[3]	[6]
$N + e^- \leftrightarrow N^+ + 2e^-$	[4][1]	[4]	[4]
$N_2 + O \leftrightarrow NO + N$	[3]	[3]	[7]
$NO + O \leftrightarrow O_2 + N$	[3]	[3]	[8]
$N + O \leftrightarrow NO^+ + e^-$	[3]	[4]	[3]
$N + N \leftrightarrow N_2^+ + e$	[3]	[4]	[4]
$O + O \leftrightarrow O_2^+ + e$	[3]	[4]	[4]
$O^+ + NO \leftrightarrow N^+ + O_2$	[3]	[3][2]	[4]
$N^+ + N_2 \leftrightarrow N_2^+ + N$	N/A	[4]	[4]
$O_2^+ + O \leftrightarrow O^+ + O_2$	N/A[3]	[4]	[4]
$N_2 + e \leftrightarrow N + N + e$	[3]	[4]	[9]
$O_2 + e \leftrightarrow O_2^+ + e$	N/A	N/A	[10]

The final variation examined within the NEQAIR code is the electron impact rates which determine the state populations in non-equilibrium (i.e. non-Boltzmann). The standard release of the NEQAIR code uses rates based upon the work of Park.[3] More recently, new rates for N, O and C have been calculated and compiled by Huo.[11] These rates are more similar to those utilized by the HARA code. These rates were converted to the NEQAIR input format for nitrogen atoms in order to evaluate the impact of these newer rates.

All together, there are 2 × 3 × 2 options which makes for 12 different variations in modelling options. All 12 variants have been examined -- a selected subset is reported here. The Park90 model with $T_e=T_t$ is chosen as a heritage option for baseline comparison. Park93 and Johnston14 are examined with $T_e=T_v$. The impact of the Huo excitation was to reduce all atomic radiation over that of Park. This result appears appropriate for more highly excited states but not the lower (3p) levels. Therefore, results from Park excitation are presented in the lower (<890 nm) wavelength regions, and Huo excitation at higher (>890 nm) wavelengths. Additionally, the effect of using a Boltzmann distribution is discussed, but not shown, for the highest pressure case.

[1] Park's text (i.e. Park90) is believed to contain a typo. The rate from Park93 is used instead.

[2] Different activation energies are given in Park's 1990 and 1993 publications. DPLR uses the rate from Park's text, even though it is likely incorrect.

[3] Park's text uses the same rate as Park93, but this rate is omitted from DPLR's chemistry input file due to a typo in Park's text.

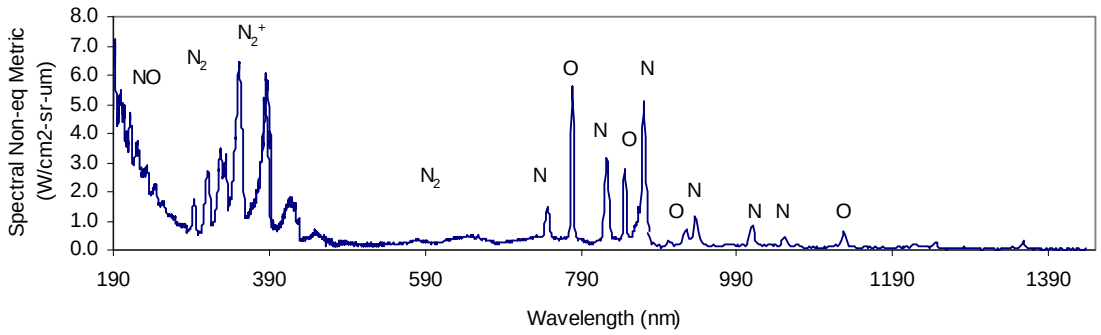

Figure 2. Non-equilibrium spectral metric at 8.33 km/s and 0.14 Torr.

4. RESULTS

The EAST data are obtained in the format of absolute radiance versus position and wavelength. An example data set is shown in Figure 1. The cross-section in the horizontal direction provides a spectral radiance while the vertical direction is the radiance versus position. The radiance versus position displays the non-equilibrium overshoot at the shock front and relaxation toward equilibrium. In order to quantify the non-equilibrium radiance, we have previously defined a metric as the integral of radiance within ±2 cm of the peak radiance.[12] When normalized by the shock tube diameter, this would have units of radiance and is equivalent to the radiance accumulated through 4 cm of the non-equilibrium "zone" when radiation is optically thin. This non-equilibrium metric may also be calculated over spectral radiance data without performing integration over wavelength. In this case it is referred to as the spectral non-equilibrium metric. The spectral non-equilibrium metric is shown in Figure 2 for one test condition, in order to identify spectral features. The spectral features present are summarized in Table III. The comparison of these values over three spectral ranges and 4 of the test conditions are shown in Figs. 3-5 at the end of the paper.

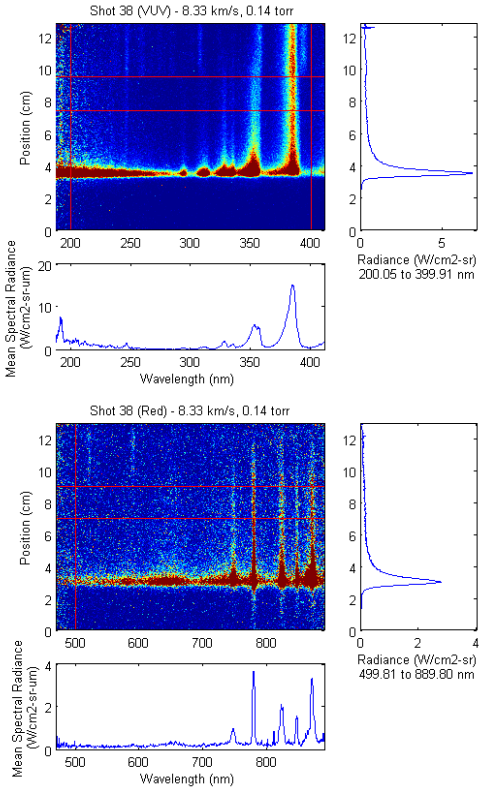

Figure 1. Sample data sets obtained in the EAST facility

Because of the large quantity of data and modelling choices, only selected comparisons are included and are discussed by wavelength range in the following sections. The Park90 model with $T_e=T_t$ and Park93 and Johnston14 with $T_e=T_v$ are chosen as representative heritage and new models for comparison of spectral features. The full set of test data, as well as the non-equilibrium metrics for the ten tests, are available on data.nasa.gov.[4]

A. VUV/UV Wavelength (190-500 nm) comparison

The 190-500 nm region primarily consists of molecular features. Because of the lack of atomic features, atomic modelling options, such as excitation rates, have little to no impact on the simulated spectra. Figure 3 shows the comparison of the non-equilibrium spectral metric at 4 of the pressures examined. Radiation features attributed to NO are underpredicted by all models, as are features attributed to the N_2 2nd Positive bands. Prediction of N_2^+ varies significantly

[4] https://data.nasa.gov/docs/datasets/aerothermodynamics/EAST/index.html, Test 59

with pressure. At the low pressure conditions of 0.01 and 0.05 Torr (not shown), the N_2^+ radiation is significantly overpredicted when using T_e=T_v. It is speculated that this result is due to the controlling temperature for associative ionization processes in DPLR leading to an overprediction of N_2^+. This phenomenon is currently under investigation. The heritage Park90 (T_e=T_t) approach matches the N_2^+ features at 0.01 Torr, but underpredicts radiance at higher pressures. At higher pressures, the N_2^+ radiation becomes more accurately predicted by the T_e=T_v models, agreeing well from 0.14-0.50 Torr, then becoming underpredicted at higher pressure. Some unmodeled CN contamination is observed near 388 nm, particularly in the 4" tube at higher pressures.[13, 14] The differences between Park93 and Johnston models are of little consequence in this range. One prediction with Boltzmann distribution (not shown) was conducted at the highest pressure examined, and this was found to capture the NO band well if the Johnston chemistry was employed, but overpredicted N_2 radiation.

Table III. Major Spectral Features in this work

Species	Feature	Transition	Major Features or Range (nm)
NO	γ, δ, ε	$(A^2\Sigma^+,C^2\Pi,D^2\Sigma^+)\rightarrow X^2\Pi$	200-300
N_2	2nd Positive	$C^3\Pi\rightarrow B^3\Pi$	337.1 357.7 380.5
	1st Positive	$B^3\Pi\rightarrow A^3\Pi$	500-750
N_2^+	1st Negative	$B^2\Sigma^+_u\rightarrow X^2\Sigma^+_g$	330.8 358.2 391.4 427.8 470.9
N		3p→3s	744.2 746.8 821.6 862.9 868.0 939.3
	NIR lines	3d→3p	1011.5 1054.0
O		3p→3s	777.2 844.6
	NIR lines	3d→3p	926.6 1128.7

B. Vis/Red Wavelength (500-890 nm) comparison

The 500-890 nm region consists of N_2 molecular excitation and atomic 3p transitions. Figure 4 shows the comparison of the non-equilibrium spectral metric in this range at 4 of the pressures examined. In order to aid the comparisons, the integral of the spectral metric is shown as a dotted line. The broad feature from 500-800 nm is attributed to N_2 1st positive radiation and is not predicted by any of the models. Several atomic features are predicted in the 500-700 nm range but are not observed in experiment. These lines generally originate from 5s and higher states of N, indicating the density of upper states is overpredicted. Lines at 777 and 845 nm are attributed to 3s states of O. The 777 nm line is underpredicted by T_e=T_v models at all conditions, while the Park 90 (T_e=T_t) model displays a fair match from 0.14-0.50 Torr, but underpredicts at high and low pressure. The agreement to the 845 nm line is similar to the 777 nm line at pressures above 0.14 Torr, but inverts at lower pressure, where the line is well matched by Park90 (T_e=T_t) but overpredicted by the T_e=T_v models. The 845 nm line is just slightly higher in energy than the 777 nm line, and the disagreement indicates errors in either the QSS prediction or the electronic temperature input to NEQAIR. The atomic N lines are generally overpredicted at the lowest pressure, but matched well from 0.05-0.50 Torr. At 0.70 Torr, the N lines are underpredicted by the Te=Tv models but matched by Park90 (T_e=T_t). One simulation with a Boltzmann distribution (not shown) was performed at 0.70 Torr and was found to provide a better match for both molecular and atomic radiation than that obtained by non-Boltzmann simulation.

C. IR Wavelength (890-1450 nm) comparison

The 890-1450 nm region consists primarily of atomic 3d transitions, though one N 3p transition of significant intensity is within this range. In this range, the Park excitation model produces a substantial overprediction. The comparisons presented in Figure 5 therefore use the Huo excitation rates. The integrated radiance is matched reasonably well by all models at 0.01 Torr, Park93/Johnston at 0.14 and 0.3 Torr and Park90 at 0.7 Torr. However, the strengths of individual features are not matched. Three lines attributable to atomic O are substantially overpredicted by all models at all pressures. This compensates under prediction in other areas such that the integrated intensity agrees. The one line attributed to the N 3p state at 939 nm is under predicted with the Huo excitation rates for Park93/Johnston, but becomes overpredicted by Park90 above 0.05 Torr. The Park excitation rates (not shown) predict this particular line better, consistent with the observations from 700-890 nm. However, the Park excitation overpredicts the intensity of the 3d states of N substantially.

5. SUMMARY

A comparison of non-equilibrium radiance at shock speeds from 7-9 km/s and pressures from 0.01-0.70 Torr has been presented. Because of the vast amount of data obtained, only a subset was presented. Comparisons are presented in terms of a non-equilibrium spectral metric, which is the integral of radiance over a 4 cm length, 2 cm in front of the shock to 2 cm behind the shock, normalized by shock tube diameter. These results are compared against predictions by the DPLR and NEQAIR codes using twelve different modelling options by varying the two-temperature model, reaction kinetics and internal excitation rates.

The comparison focuses on radiation from NO, N_2, N_2^+ and atomic N and O. The NO and N_2 radiation is underpredicted by all models at all conditions. N_2^+ radiation is overpredicted at low pressure when T_e=T_v. N_2^+ radiation is predicted well at low pressure with the heritage model (Park 90 and T_e=T_t) but is better matched by either Park93 or Johnston kinetics and T_e=T_v at intermediate pressures (0.14-0.50 Torr). At higher pressures, the N_2^+ non-equilibrium is underpredicted by all models. The Boltzmann distribution at the highest pressure improves predictions of NO (with Johnston's chemistry) and the lower-energy N_2 band, suggesting updates to the molecular non-Boltzmann model are required. Atomic line radiation predictions are mixed. The lowest energy states of N (3p) are predicted well from 0.05-0.50 Torr when T_e=T_v is employed. The 3p states of atomic O are overpredicted by the T_e=T_v models but predicted well at intermediate pressure ranges by the heritage model. Higher energy N and O lines, however, are overpredicted. The excitation rates recommended by Huo and implemented in NEQAIR were found to significantly reduce all atomic emission. While this reduction may be appropriate for the higher energy states, it resulted in substantial underprediction of important 3p states. Future work will focus on refinements to chemical reaction and excitation models to improve predictions.

6. REFERENCES

1. Brandis, A. M., Johnston, C. O., Cruden, B. A., Prabhu, D., and Bose, D., "Uncertainty Analysis and Validation of Radiation Measurements for Earth Reentry," Journal of Thermophysics and Heat Transfer, Vol. 29, No. 2, 2015, pp. 209-221.

2. Cruden , B. A., "Absolute Radiation Measurements in Earth and Mars Entry Conditions," RTO-EN-AVT-218, 2014.

3. Park, C., Nonequilibrium Hypersonic Aerothermodynamics, New York: John Wiley & Sons, 1990.

4. Park, C., "Review of chemical-kinetic problems of future NASA missions. I - Earth entries," Journal of Thermophysics and Heat Transfer, Vol. 7, No. 3, 1993, pp. 385-398.

5. Johnston, C. O., "Study of Aerothermodynamic Modelling Issues Relevant to High-Speed Sample Return Vehicles," VKI 2013-AVT-218.

6. Johnston, C. O., and Brandis, A. M., "Modelling of nonequilibrium CO Fourth-Positive and CN Violet emission in CO2–N2 gases," Journal of Quantitative Spectroscopy and Radiative Transfer, Vol. 149, 2014, pp. 303-317.

7. Fujita, K., Yamada, T., and Ishii, N., "Impact of Ablation Gas Kinetics on Hyperbolic Entry Radiative Heating," 2006.

8. Bose, D., and Candler, G. V., "Thermal rate constants of the O-2+ N-> NO+ O reaction based on the (2) A'and (4) A'potential-energy surfaces," Journal of Chemical Physics, Vol. 107, No. 16, 1997, pp. 6136-6145.

9. Bourdon, A., and Vervisch, P., "Study of a low-pressure nitrogen plasma boundary layer over a metallic plate," Physics of Plasmas (1994-present), Vol. 4, No. 11, 1997, pp. 4144-4157.

10. Teulet, P., Gonzalez, J., Mercado-Cabrera, A., Cressault, Y., and Gleizes, A., "One-dimensional hydro-kinetic modelling of the decaying arc in air–PA66–copper mixtures: I. Chemical kinetics, thermodynamics, transport and radiative properties," Journal of Physics D: Applied Physics, Vol. 42, No. 17, 2009, p. 175201.

11. Huo, W. M., Liu, Y., Panesi, M., Wray, A., and Carbon, D. F., "Electron-Impact Excitation Cross Sections for Modelling Non-Equilibrium Gas," AIAA Paper 2015-1896.

12. Cruden, B. A., "Radiance Measurement for Low Density Mars Entry," AIAA Paper 2012-2742.

13. Cruden, B. A., Martinez, R., Grinstead, J. H., and Olejniczak, J., "Simultaneous Vacuum Ultraviolet through Near IR Absolute Radiation Measurement with Spatiotemporal Resolution in an Electric Arc Shock Tube," AIAA Paper 2009-4240.

14. Bose, D., McCorkle, E., Bogdanoff, D., and Gary A. Allen, J., "Comparisons of Air Radiation Model with Shock Tube Measurements," AIAA 2009-1030.

a) 0.01 Torr

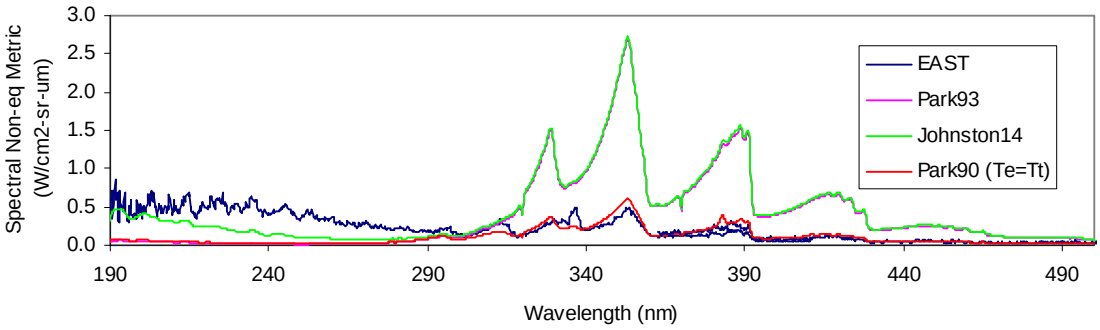

b) 0.14 Torr

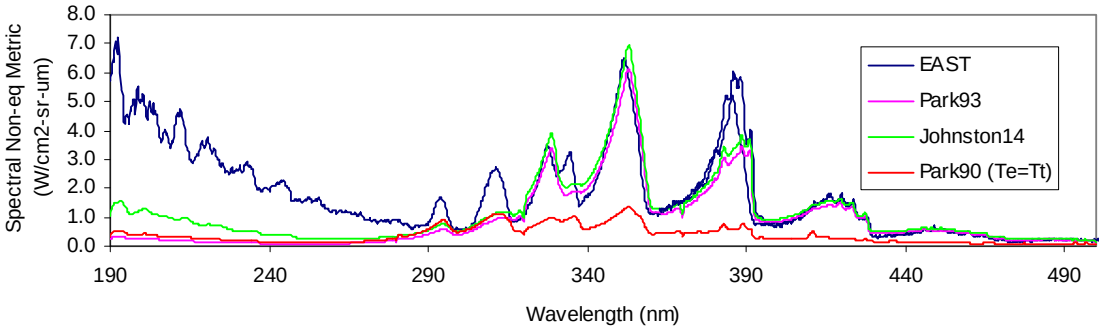

c) 0.30 Torr

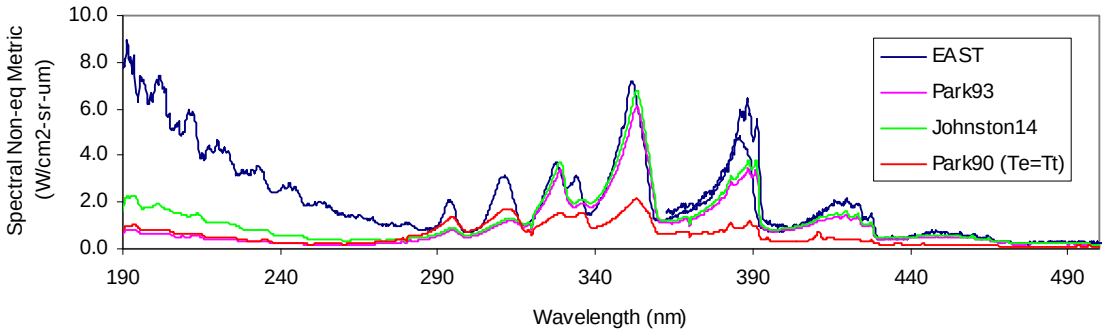

d) 0.70 Torr

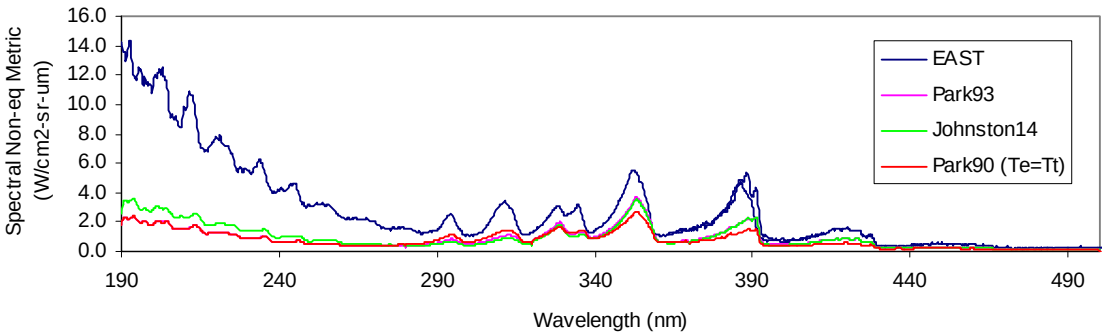

Figure 3. Spectral non-equilibrium metrics from 190-500 nm at four pressures.

a) 0.01 Torr

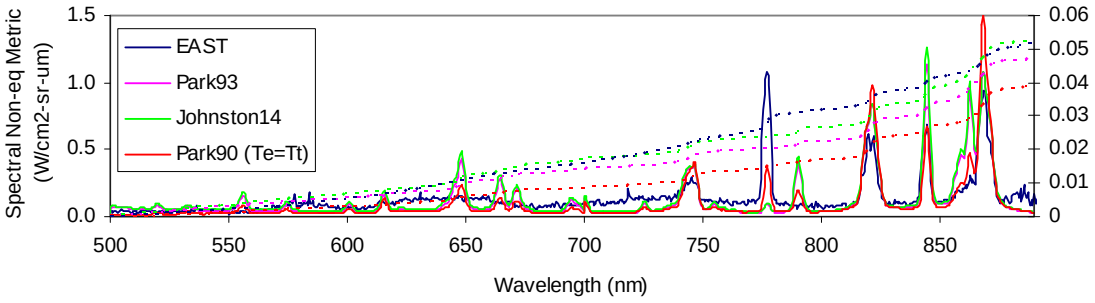

b) 0.14 Torr

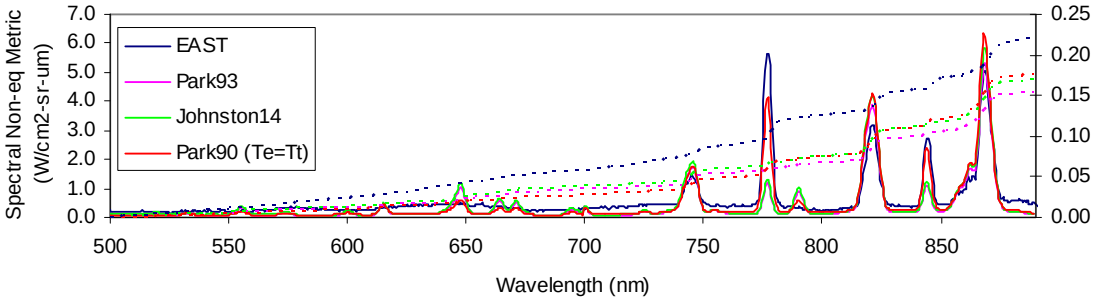

c) 0.30 Torr

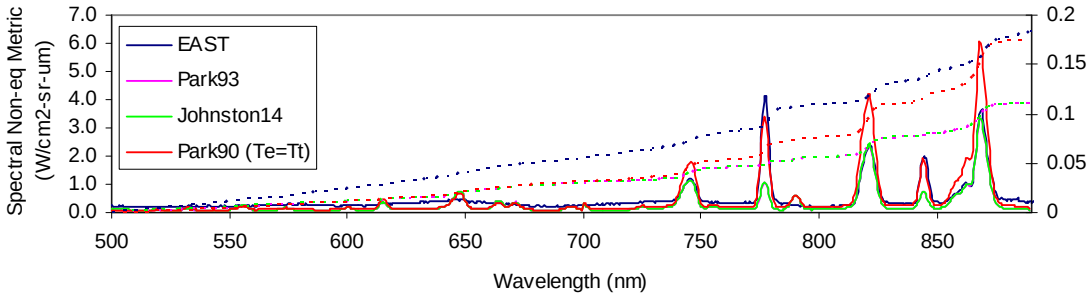

d) 0.70 Torr

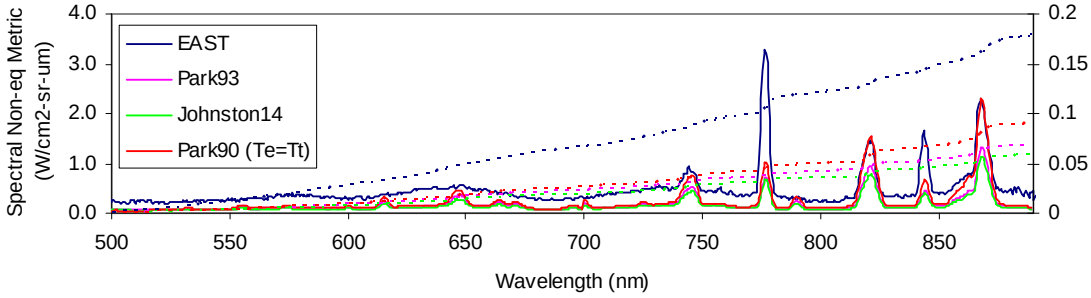

Figure 4. Spectral non-equilibrium metrics from 500-890 nm.

a) 0.01 Torr

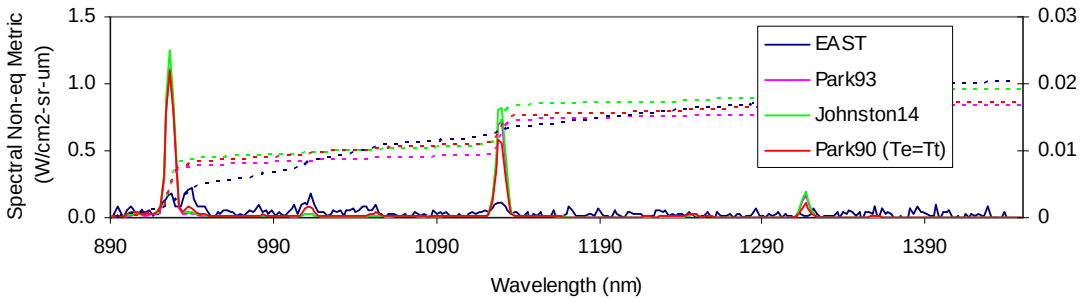

b) 0.14 Torr

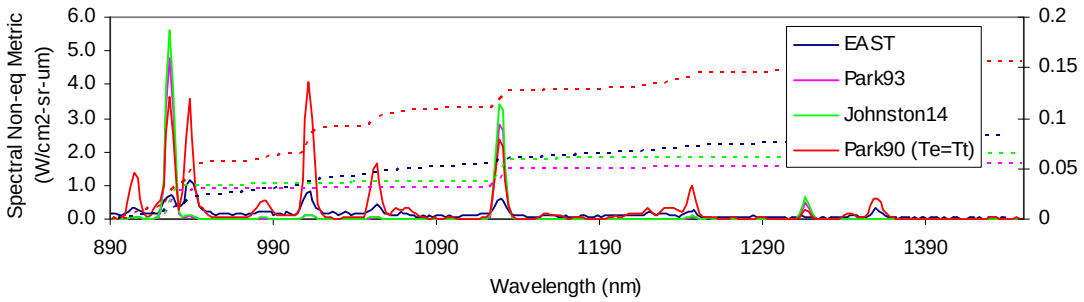

c) 0.30 Torr

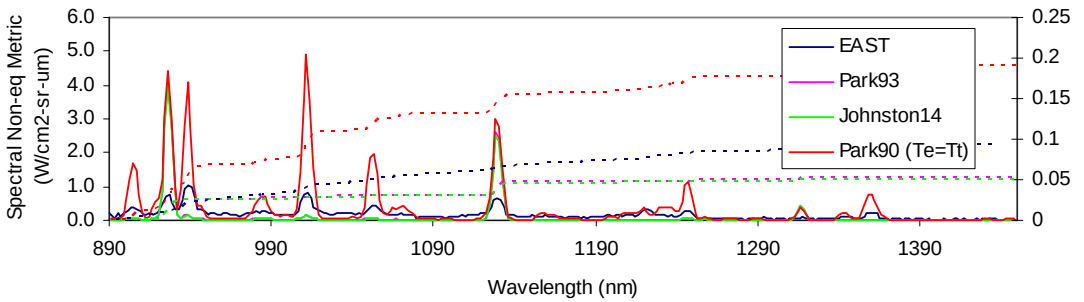

d) 0.70 Torr

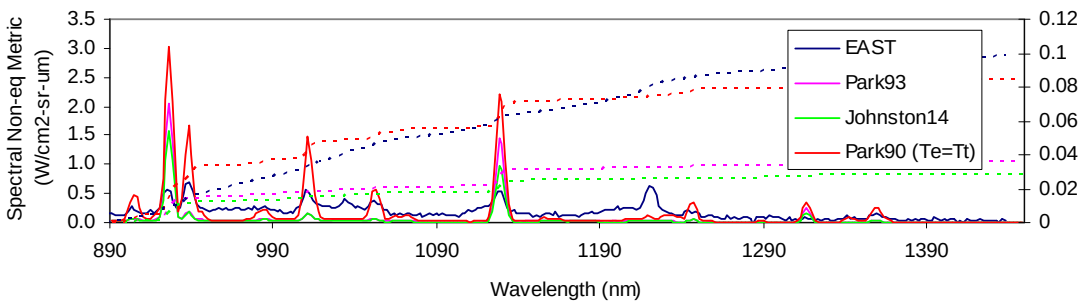

Figure 5. Spectral non-equilibrium metrics from 890-1450 nm.